

Caryinite revisited

T. SCOTT ERCIT

Mineral Sciences Section, Canadian Museum of Nature, Ottawa, Ontario, Canada K1P 6P4

Abstract

Caryinite from Långban, Sweden is associated with barite, richterite, manganberzeliite, hedyphane, sarkinite or eveite, and an exsolved ferromite-like mineral. The crystal structure of caryinite, space group $I2/a$, a 6.855(2), b 13.147(3), c 11.479 (4) Å, β 98.97°, V 1022.0(5) Å³, has been refined to a conventional $R = 3.5\%$ using 1295 observed [$F > 3\sigma(F)$] reflections. Caryinite is isostructural with alluaudite and shows the following key features: (1) Pb is ordered at $X2$, Mg is ordered at $M2$, Mn is disordered over $M1$ and $M2$, Ca is disordered over $M1$ and $X1$ and Na is disordered over $X1$ and $X2$, and (2) the $X1$ and $O2$ atoms of the $X1$ polyhedron show positional disorder. With the above site preferences taken into consideration, the assignment rules of Moore and Ito (1979) can now be used to accurately predict site occupancies for caryinites and arseniopleites using chemical data only. On the basis of the general structural formula $X2X1M1M2_2[AsO_4]_3$ ($Z = 4$), caryinite is (Na, Pb) (Ca, Na) Ca (Mn, Mg)₂ [AsO₄]₃; the analogous formula for arseniopleite is Na(Ca,Na)Mn(Mn,Mg)₂[AsO₄]₃. Caryinite has Ca dominant at $M1$; by analogy, arseniopleite should have Mn dominant at $M1$.

KEYWORDS: caryinite, crystal structure, arsenate, alluaudite, arseniopleite, Långban, Sweden.

Introduction

Caryinite was discovered by Lundström (1874) at the Långban mine, near Filipstad, Varmland, Sweden. Several studies of the chemistry and X-ray diffraction properties of the mineral followed; these are summarised by Boström (1957). More recently, Moore (1971) showed alluaudite and caryinite to be isostructural, Dunn and Peacor (1987) suggested general formulae for caryinite and its relative arseniopleite based on new electron microprobe data, and Keller *et al.* (1981) and Keller and Hess (1988) refined the structures of synthetic and natural arsenate allaudites.

Dunn and Peacor (1987) showed the diffraction properties of caryinite and arseniopleite to be completely compatible with those of alluaudite; there were no space group or metric violations suggestive of additional cation ordering, such as with wyllieite and bobfergusonite (Moore and Molin-Case, 1974; Ercit *et al.* 1986). However, the formulae given by Dunn and Peacor (1987) for both caryinite and arseniopleite open the possibility for the additional cation sites; the $X2$ site sums for caryinite and arseniopleite are exceeded by 0.37 and 0.28 cations per unit cell, respectively. The $X2$ site of alluaudite was discovered in a similar manner (Moore and Molin-Case, 1974). A structure refinement was done with this consideration in mind, and was also

directed toward resolving the uncertainties of Ca and Pb ordering in the alluaudite structure.

Experimental

The caryinite sample used in the study was borrowed from the Smithsonian Institution, sample R6508. A 0.5 cm-long cleavage fragment was extracted from the sample; part of the fragment was mounted in epoxy for electron microprobe analysis; the other part was used for X-ray diffraction experiments.

Chemical analysis was done with a JEOL 733 electron microprobe using Tracor-Northern 5500 and 5600 automation. The instrument was operated at 15 kV; the sample current was 20 nA; data were collected for 50 s or to 0.5% precision, whichever was attained first. The beam diameter was conventionally set at 20 µm so as to minimise sample degradation; however, for the analysis of a ferromite-like phase, a point-focused beam had to be used. Standards were: synthetic tephroite (Mn), almandine (Fe), diopside (Ca, Mg), synthetic sanbornite (Ba), albite (Na), synthetic arsenate-alluaudite $AgCo_3H_2[AsO_4]_3$ (As), apatite (P) and VP_2O_7 (V). For caryinite, the following were also sought but were not detected: Si, Sr, F. All data were reduced with a conventional ZAF routine in the Tracor-Northern TASK series of programs.

Preliminary X-ray examination was done with a Supper precession camera using Zr-filtered MoK α radiation. Both zero- and first-level photographs were taken for settings with X and Y as the precession axes; no violations of I centring or of caryinite metricity were observed. Intensity data were collected with a Nicolet R3m four-circle diffractometer at the University of Manitoba, using the experimental method of Ercit *et al.* (1986). Twenty-five intense reflections were used to centre the crystal; least-squares refinement of the setting angles gave the unit-cell parameters in Table 1, and the orientation matrix used for data collection. One asymmetric unit of data was collected to a maximum $\sin \theta/\lambda$ of 0.7035, which gave the 1487 unique reflections, of which 1295 were considered observed [$F > 3\sigma(F)$].

Absorption correction was done with the empirical XEMP program in the SHELXTL package of programs. The correction was based on ψ -scan data collected on ten reflections, assuming a pseudo-ellipsoidal shape for the crystal, and resulted in a reduction of the merging R for the ψ -scan set from 6.8% to 3.5%.

Data reduction (correction for $L \cdot p$ and background effects) was done with the SHELXTL package of programs. Crystal-structure analysis and refinement were done with the SHELXTL PC package of programs. Scattering curves for neutral atoms, together with anomalous dispersion corrections were taken from Cromer and Mann (1968) and Cromer and Liberman (1970), respectively.

Results

Microprobe study. The caryinite fragment examined by electron microprobe (Table 2) has a variety of associated mineral phases. These are richterite, barite and manganberzeliite as coprecipitates, hedyphane and sarkinite or eveite as fracture fillings and what would seem to be a Sr-free variety of ferromite as exsolution lamellae in the caryinite. The lamellae of this unknown ferromite-like phase were too small for X-ray diffraction examination, and too narrow for a

high-quality microprobe analysis. Nevertheless, an analysis of the widest lamella is presented in Table 2; the phase shows apparent Ca₅[PO₄]₂[AsO₄](OH) stoichiometry, suggesting complete As-P order, as one might expect for such an intermediate composition. The volume percentage of this phase is small, less than 5%; the implication is that at high temperatures, caryinite can tolerate slightly greater amounts of P in its structure.

Structure refinement. The refinement of the caryinite structure started with an alluaudite model, general formula $X_2X_1M_1M_2[AsO_4]_3$ (Moore, 1971; Moore and Molin-Case, 1974), set in $I2/a$ (Ercit *et al.*, 1986). Site occupancies were derived from the electron microprobe analysis (Table 2) on the basis of model proposed by Dunn and Peacor (1987); most noteworthy of this model is the assignment of Pb to X1, of Na to X2, and the splitting of Ca between X1, X2 and M1. A few cycles of refinement showed a surplus of scattering from X2, matched by similar deficit from X1, indicating that Pb is located at X2. After a few more cycles of refinement, the microprobe constraints for site occupancies were removed; the unconstrained refinement did not match microprobe results well, indicating that some site assignments were incorrect. In particular, it was found that: (1) X2 cannot be occupied by both Ca and Pb. An acceptable value for the fractional occupancy of Pb at X2 can only result if a lighter scatterer than Ca is present at X2; i.e. Na, not Ca, is the associate of Pb at X2. (2) X1 hosts considerably less Na and more Ca than first anticipated. This indicates that the initial errors in site assignments for X1 and X2 can be compensated by reassigning constituents between the sites; the constituents of M1 and M2 need not be involved in order to remedy the situation.

At this stage the X-site occupants were adjusted to match the above considerations and several cycles of refinement were carried out, without microprobe constraints. The fractional occupancy of Pb at X2 and the combined fractional occupancies of Na at X1 and X2 were found to be close to microprobe measurements for these two elements, confirming the correctness of the

Table 1. Miscellaneous information for caryinite

a (Å)	6.855(2)	Space group	$I2/a$
b	13.147(3)	Crystal size (mm)	0.10 x 0.12 x 0.10
c	11.479(4)	μ (cm ⁻¹), radiation	186, MoK α
β (°)	98.97(2)	Total F_o , Obs. F_o	1487, 1295
V (Å ³)	1022.0(5)	Final R , wR (%)	3.54, 3.66
R factors:		$R = \Sigma(F_o - F_c) / \Sigma F_o $	
		$wR = [\Sigma w(F_o - F_c)^2 / \Sigma w F_o ^2]^{1/2}$, $w = 1$	

Table 2. Compositions of caryinite and ferromite-like phase, Långban, Sweden

	Caryinite	Ferromite-like Phase
Na ₂ O wt. %	4.82(5)	0.11(1)
CaO	10.82(8)	47.73(34)
BaO	0.17(3)	----
PbO	12.73(42)	1.02(17)
MgO	3.24(3)	0.22(1)
MnO	17.90(15)	1.23(4)
FeO	0.10(2)	----
P ₂ O ₅	0.95(3)	24.40(14)
V ₂ O ₅	0.24(2)	----
As ₂ O ₅	48.84(34)	19.36(15)
H ₂ O*		1.56
	99.81	95.63
<i>Cations per formula unit</i>		
Na	1.041	0.021
Ca	1.305	4.923
Ba	0.007	----
Pb	0.387	0.026
Mg	0.543	0.032
Mn	1.707	0.100
Fe	0.010	----
P	0.091	1.989
V	0.018	----
As	2.891	0.974
	8.000	8.065
O	11.978	

Caryinite: average of two analyses. Statistically most-probable formula calculated with LAGRAN program (Dollase and Newman, 1984); constraints: cation sum = 8, tetrahedral cation sum = 3.

Ferromite-like phase: formula on a basis of 12(O) + 1(OH). *H₂O calculated for stoichiometry.

X-site assignments. At this point the ordering behaviour of P was examined; P was found to be equally distributed between the As1 and As2 sites, so the fractional occupancies of these sites were fixed to reflect this conclusion, at microprobe-determined values for As and P (and V). All displacement parameters were eventually converted to anisotropic; this model converged at values of $R = 3.52$, $wR = 3.70\%$. The displacement parameters for X1 and O2 were of sufficient magnitude and anisotropy to indicate positional disorder about these sites. For the new model, X1 was split away from its inversion centre in a sense compatible with its apparent vibration ellipsoid. Treatment of O2 was not simple as O2 occupies a general position—O2 was split into two general positions; refinement was constrained so that each component of the split model was equally but oppositely displaced from the last refined position for O2 in the anisotropic model. Refinement of this final model converged at values statistically indistinct from the fully anisotropic model ($R = 3.54$, $wR = 3.66\%$ for all observed data; $R = 4.23$, $wR = 4.16\%$ for all 1487 data).

The refined values of the positional parameters and the anisotropic and equivalent isotropic U 's for the atoms of the caryinite structure are given in Table 3. The refined site occupancies are given

in Table 4. The observed and calculated structure factors for the final model are given in Table 5.*

Description of the structure. The average features of the caryinite structure are shown in Fig. 1. It is topologically identical to the alluaudite structure; it is a layer structure, with alternations of strongly-bonded and weakly-bonded layers along Y . The strongly-bonded layer (Fig. 1a) consists of staggered chains of edge-sharing M1, M2 octahedra cross-linked by AsO₄ tetrahedra. The weakly-bonded layer (Fig. 1b) consists of straight chains of either face-sharing X1 polyhedra or edge-sharing X2 polyhedra; these chains are infinite along X , and alternate in type along Z .

Bond lengths are given in Table 6. The bond lengths confirm the site assignments of Table 4, which together stress that cation ordering in the caryinite structure is strongly driven by cation size. The ranking in order of decreasing size preference is $X2 > X1 > M1 > M2$. One can predict site populations on the basis of effective cation radius quite well. Mg, the smallest cation, is assigned to M2. The remainder of M2 is assigned as Mn, and the excess Mn is assigned to

* Available on request from the Mineralogical Society office.

Table 3. Positional and thermal parameters for caryinite

	<i>x</i>	<i>y</i>	<i>z</i>	<i>U</i> ₁₁	<i>U</i> ₂₂	<i>U</i> ₃₃	<i>U</i> ₂₃	<i>U</i> ₁₃	<i>U</i> ₁₂	<i>U</i> _{eq}
X1	0.0268(4)	0.0023(3)	0.5137(3)							170
X2	1/4	0.0246(1)	0	244(5)	282(5)	266(5)	0	91(3)	0	258(3)
M1	1/4	0.7350(1)	0	202(8)	149(7)	165(7)	0	11(5)	0	174(4)
M2	0.0849(2)	0.1575(1)	0.2229(1)	158(5)	178(5)	176(5)	8(4)	30(4)	-13(4)	170(3)
As1	1/4	0.2836(1)	0	162(4)	163(4)	169(4)	0	67(3)	0	160(2)
As2	0.1059(1)	0.8906(1)	0.2342(1)	152(3)	162(3)	171(3)	4(2)	59(2)	-3(2)	158(2)
O1	0.0775(6)	0.2083(4)	0.0435(4)	189(20)	345(25)	196(20)	4(18)	78(16)	-105(18)	238(13)
O2	0.1591(9)	0.1272(7)	0.4019(8)							200
O2'	0.1076(9)	0.1401(7)	0.4027(8)							200
O3	0.2745(6)	0.8326(3)	0.1644(4)	169(20)	193(20)	285(22)	-46(17)	99(17)	-8(16)	209(12)
O4	0.1902(7)	0.9076(4)	0.3786(4)	273(22)	257(22)	191(20)	-16(17)	55(17)	7(18)	238(13)
O5	0.1019(6)	0.3208(3)	0.2773(4)	159(20)	235(21)	263(22)	-7(17)	74(17)	5(16)	214(12)
O6	0.0520(7)	0.0021(3)	0.1635(4)	248(22)	172(19)	248(21)	24(17)	65(17)	-1(17)	220(12)

All *U*'s are Å² × 10⁴

Table 4. Site occupancies: microprobe assignments versus structure refinement

Site:	X1		X2		M1		M2	
Structure	0.62(2)	Ca	0.616(3)	Na	0.67(2)	Ca	0.72(1)	Mn
Refinement:	0.38(2)	Na	0.384(3)	Pb	0.33(2)	Mn	0.28(1)	Mg
Electron	0.56	Ca	0.61	Na	0.74	Ca	0.73	Mn
Microprobe:	0.44	Na	0.39	Pb	0.26	Mn	0.27	Mg

M1. The remainder of M1 is assigned as Ca, and the excess Ca is assigned to X1. Pb, the largest cation is assigned to X2, and Na is split between X1 and X2. Table 4 shows the result of applying this procedure to the electron microprobe analysis of the studied caryinite sample: the site populations derived from the microprobe analysis match the values from the structure refinement to within a few standard deviations. It is important to note that Na, Mg and Mn show identical site preferences in both the caryinite structure and the structures of alluaudite and its derivatives; i.e. the same site assignment rules seem to apply to both phosphate and arsenate alluaudites (see Moore and Ito, 1979 for extended rules). As Ca has not yet been found in great abundance in the phosphate alluaudites, one must look to the arsenate alluaudites for clues to its behaviour; the present study suggests that for Mn-rich phosphate alluaudites, Ca will be disordered over X1 and M1.

A bond-valence analysis for the caryinite structure is shown in Table 7. The bond-valence sums match predictions reasonably well. For comparison, the predicted sums for the X sites are: X1 1.62, X2 1.38 *v.u.*; the individual predicted sums for the M sites are 2 *v.u.*, for the As sites are 5 *v.u.*, and for the O sites are 2 *v.u.* No amount of shifting of site constituents maximises agreement

between the observed and calculated values, further attesting to the correctness of the site assignments. The magnitude of disagreement between the observed and predicted sums for the X2 site seems large; however, there seems to be no obvious structural answer for this discrepancy.

The X1 site. Although positional disorder has not been noted for X1 in previous refinements of the alluaudite structure, it has been noted for X1 analogues in derivatives of the alluaudite structure (wyllicite; Moore and Molin-Case, 1974; bobfergusonite; Ercit *et al.* 1986). To understand positional disorder in caryinite, it is important to note that (1) both X1 and O2 are disordered; (2) O2 is one of the coordinating oxygen atoms in the X1 polyhedron; (3) for the *average* caryinite structure, i.e. ignoring positional disorder, the longest X1–O bond is the X1–O2 bond; (4) for this longest X1–O2 bond, both the O2–O2 separation and the X1–X1 separation parallel the bond direction; and (5) the magnitude of X1–X1 separation is comparable to that of the O2–O2 separation, 0.45 Å versus 0.40 Å, respectively. All of the above points suggest that O2 disorder is dependent upon X1 disorder. Presumably, X1 disorder results from the inability of the oxygen atoms of the X1 polyhedron to collapse to a sufficient distance to satisfy the bond-valence

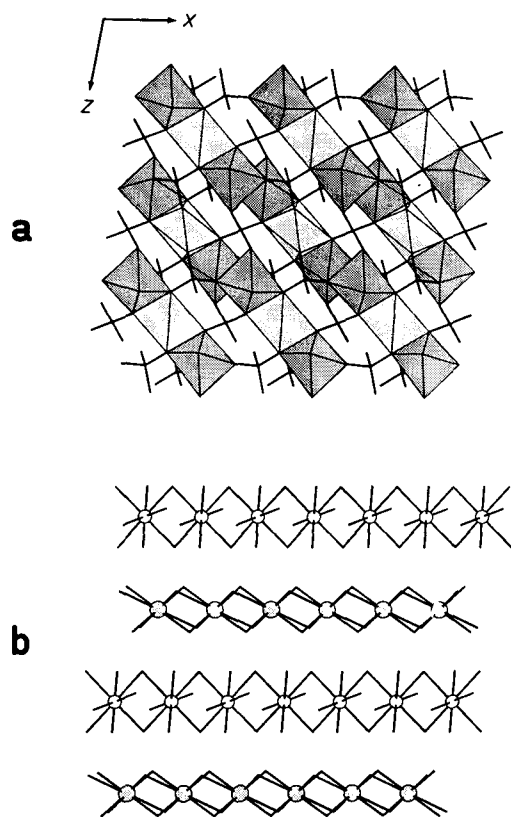


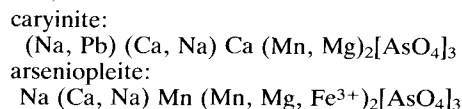
FIG. 1. The caryinite structure as projected down *Y*. (a) Strongly-bonded layer. *M*-cation octahedra link via edge-sharing to form staggered chains parallel to $[101]$. The *M1* octahedron is shown in light stippling and the *M2* octahedron is shown in dark stippling; for clarity only the P-O bonds of P tetrahedra are shown. (b) Weakly-bonded layer. The *X1* polyhedron is shown in its average configuration. *X1* polyhedra share faces and *X2* polyhedra share edges to form two types of straight chain parallel to *X*. *X1* is shown as a shaded circle, *X2* is shown as an unshaded circle.

requirements of the *X1* cation; consequently, *X1* is displaced from the inversion centre toward one side of the polyhedron in the direction of a coordinating O2 atom; the pertinent O2 atom is drawn toward the displaced *X1* cation, with all displacements resulting in an improved set of bond valences for the *X1* polyhedron. When averaged over a crystal, *X1* is [8]-coordinated; however, on a unit-cell scale *X1* actually assumes [7]-coordination (Fig. 2). The lack of any reflections violating $I2/a$ symmetry or alluaudite-cell

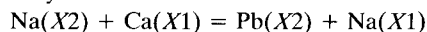
metricity indicates that the positional displacements of *X1* and O6 are not ordered; however, one cannot help but wonder if the apparent violations of *I* centring noted by Boström (1957) (but not observed in this study or by Dunn and Peacor, 1987) indicate that some caryinites show ordered displacements of *X1* and O6.

Status of caryinite and arsenioleite. It is important to note that the electron microprobe analysis and the results of the structure refinement do not confirm the presence of an extra cation site. P. J. Dunn (pers. comm.) supplied unpublished analyses of arsenioleites and caryinites, including caryinite R6508; his analysis of R6508 is very similar to the result in Table 2 with the exception of Mn and As. Presumably the slightly high cation sums for caryinite and arsenioleite in Dunn and Peacor (1987) are, in part, due to unavoidable errors in ZAF calculations for the available standards. By comparison with the results of the present study, it is tempting to suggest correction factors for the data of Dunn and Peacor (1987); however, as caryinite R6508 is inhomogeneous, this does not seem to be a wise course of action.

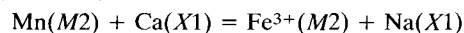
Consideration of the results of the structure refinement with the chemistry of caryinite and arsenioleite suggests the following idealized formulae (general formula $X_2X_1M_1M_2[AsO_4]_3$, $Z = 4$):



All analyses of caryinites and arsenioleites to date show that both species host intermediate amounts of Na and Ca; the mean ratios of Na:Ca are caryinite 0.44, arsenioleite 0.22 (Långban), 0.42 (Sjö, Sweden). The mechanism most responsible for introducing Na at *X1* differs between the species. For caryinite the introduction of Na at *X1* is mainly due to Pb at *X2*:



For arsenioleite, Na enters *X1* mainly in response to Fe^{3+} at *M2*:



Dominance of Na at *X1* has the potential of causing nomenclature problems. The problem hasn't been encountered yet: all caryinites and arsenioleites analysed to date have Ca dominant at *X1*. Furthermore, the precedent set by Moore and Ito (1979) for the phosphate alluaudites exists for consultation should the line be crossed.

By the criteria used by Moore and Ito (1979) for the phosphate alluaudites, and as Dunn and Peacor (1987) proposed, caryinite and arsenio-

Table 6. Bond lengths for caryinite

X1-O2	2.351(9)	M1-O1	2.344(4) x2	As1-O1	1.677(5) x2
-O2	2.419(9)	-O3	2.267(5) x2	-O2*	1.685(6) x2
-O2	2.760(8)	-O4	2.334(5) x2	<As1-O>	1.681
-O4	2.399(6)	<M1-O>	2.315		
-O4	2.392(6)				
-O4	2.470(5)				
-O4	2.832(5)				
<X1-O>	2.518 Å				
X2-O1	3.141(5) x2	M2-O1	2.157(5)	As2-O3	1.688(5)
-O3	2.768(5) x2	-O2*	2.068(6)	-O4	1.682(4)
-O6	2.499(5) x2	-O3	2.133(4)	-O5	1.682(4)
-O6	2.592(4) x2	-O5	2.234(5)	-O6	1.689(4)
<X2-O>	2.750	-O5	2.166(5)	<As2-O>	1.685
		-O6	2.155(5)		
		<M2-O>	2.152		

O2* = <O2, O2'>

Table 7. Bond-valence table for caryinite

	O1	O2	O3	O4	O5	O6	SUM
X1		0.28 /2↓ 0.24 /2↓ 0.12		0.25 /2↓ 0.26 /2↓ 0.21 /2↓ 0.10 /2↓			1.46
X2	0.12 x2→		0.06 x2→			0.22 x2→ 0.18 x2→	1.16
M1	0.30 x2→		0.35 x2→	0.30 x2→			1.90
M2	0.34	0.43	0.36		0.28 0.33	0.34	2.08
As1	1.24 x2→	1.22 x2→					4.92
As2			1.21	1.23	1.23	1.20	4.87
SUM	2.00	2.03	1.98	1.94	1.84	1.94	

- bond valences (v.u.) from curves of Brown (1981)

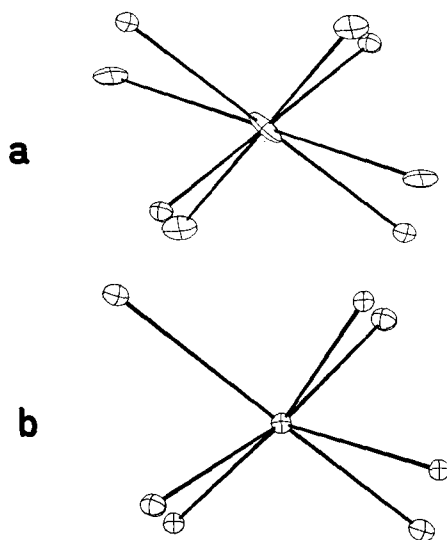


FIG. 2. The average (a) and actual (b) coordination of X1. Averaged over a crystal, X1 has apparent [8]-coordination. However, on a unit-cell scale X1 is displaced from its inversion centre, toward one of the two most-distant oxygen atoms of the coordination (O2). O2 is similarly displaced toward X1, resulting in a shortening of the X1-O2 bond from 3.15 to 2.76 Å, and in reducing the coordination of X1 from eightfold to sevenfold.

pleite are separate species; caryinite has Ca dominant at M1; by analogy, arsenioleite has Mn dominant at M1.

Acknowledgements

I thank J. S. White, formerly of the Smithsonian Institution, for loan of the caryinite sample and F. C. Hawthorne, University of Manitoba, for the use of the four-circle diffractometer. I especially thank P. J. Dunn of the Smithsonian Institution for providing unpublished analyses of caryinite and arsenioleite samples, and for a review of an earlier version of the manuscript; note, however, that all of the opinions of the present author are not necessarily shared by Dr Dunn. Financial support for this work was in the form of a Canadian Museum of Nature research stipend.

References

- Boström, K. (1957) The chemical composition and symmetry of caryinite. *Arkiv Mineral. Geol.*, **4**, 333-6.
- Brown, I. D. (1981) The bond-valence method: an empirical approach to chemical structure and bonding. In *Structure and Bonding in Crystals II* (M. O'Keeffe and A. Navrotsky, eds.). Academic Press, New York.
- Cromer, D. T. and Liberman, D. (1970) Relativistic calculation of anomalous scattering factors for X-rays. *J. Chem. Phys.*, **53**, 1891-8.

- and Mann, J. B. (1968) X-ray scattering factors computed from numerical Hartree-Fock wave functions. *Acta Cryst.*, **A24**, 321–4.
- Dollase, W. A. and Newman, W. I. (1984) Statistically most probable stoichiometric formulae. *Amer. Mineral.*, **69**, 553–6.
- Dunn, P. J. and Peacor, D. R. (1987) New data on the relation between caryinite and arseniopleite. *Mineral. Mag.*, **51**, 281–4.
- Ercit, T. S., Hawthorne, F. C., and Cerny, P. (1986) The crystal structure of bobfergusonite. *Can. Mineral.*, **24**, 605–14.
- Keller, P., Riffel, H., Zettler, F., and Hess, H. (1981) $\text{AgCo}_3\text{H}_2(\text{AsO}_4)_3$ und $\text{AgZn}_3\text{H}_2(\text{AsO}_4)_3$. Darstellung und Kristallstruktur. Ein weiterer neuer Arsenat-Struktur-typ. *Zeits. Anorg. Allg. Chem.*, **474**, 123–34.
- and Hess, H. (1988) Die Kristallstrukturen von O'Danielit, $\text{Na}(\text{Zn}, \text{Mg})_3\text{H}_2(\text{AsO}_4)_3$, un Johillerit, $\text{Na}(\text{Mg}, \text{Zn})_3\text{Cu}(\text{AsO}_4)_3$. *Neues Jahrb. Mineral. Mh.*, 395–404.
- Lundström, C. H. (1874) Koryinit från Långbanshyttan i Vermland. *Geolog. Fören. Förh. i Stokholm*, **2**, 178, 223.
- Moore, P. B. (1971) Crystal chemistry of the alluaudite structure type: contribution to the paragenesis of pegmatite phosphate giant crystals. *Amer. Mineral.*, **56**, 1955–75.
- and Ito, J. (1979) Alluaudites, wyllieites, arrojaudites: crystal chemistry and nomenclature. *Mineral. Mag.*, **43**, 227–35.
- and Molin-Case, J. (1974) Contribution to pegmatite phosphate giant crystal paragenesis. II. The crystal chemistry of wyllieite, $\text{Na}_2\text{Fe}^{2+}_2\text{Al}[\text{PO}_4]_3$, a primary phase. *Amer. Mineral.*, **59**, 280–90.

[Manuscript received 30 July 1992]